Investigation of Symmetric Thermal Decay and Asymmetric Radiative Collapse of NBI Heated Plasma on LHD

Yuhong Xu, B. J. Peterson, S. Sudo, T. Tokuzawa, K. Narihara, M.Osakabe, M.Goto, S. Sakakibara, K. Tanaka, K. Kawahata, K. Tsumori, K. Ikeda, S. Kubo, H. Idei, J. Miyazawa, K. Y. Watanabe, K. Nishimura, A. Kostrioukov, H. Yamada, O. Kaneko, N. Ohyabu, K. Komori and the LHD Experimental Group

National Institute for Fusion Science, Toki-shi, Gifu-ken 509-5292, Japan

1. Introduction

In both tokamak and helical plasmas the maximum achievable density is limited[1,2]. Increasing the density induces an increase in impurity radiation and thus a radiative collapse via a thermal instability[3]. In tokamaks, both the poloidally symmetric radiation belt and the asymmetric MARFE(multifaceted asymmetric radiation from the edge) have been observed[1,4]. In helical devices, the issues regarding the density limit and radiative collapse have also been studied intensively [2,5-7]. On LHD, a MARFE-like radiation profile has been observed[7]. In this paper, the basic features, including the radiation structures, in the decay and collapse discharges on LHD are compared. The time evolutions of the radiation profile in the collapse discharges are investigated.

2. Experimental setup and diagnostics

The Large Helical Device(LHD) is a large superconducting heliotron system with a set of l/m=2/10 helical coils. The experiments subjected to this work were conducted under conditions of R/a=3.6~3.75m/0.6m, B_t=1.5~2.75T, n_e=0.6~7.0$\times 10^{19}$m^{-3} and $T_e(T_i)$ = 0.5~2 keV. The total plasma radiation profile is measured by a multi-channel bolometer array viewing the vertically elongated cross-section of the plasma[7].

3. Basic features of the decay and collapse of NBI heated plasmas on LHD

In LHD, the NBI heated discharges are terminated in two ways: (a) thermal decay(TD) after the termination of NBI; (b)radiative collapse(RC) during the NBI. The typical discharge waveforms of the TD and RC shots are displayed in Fig. 1. The figure shows that the plasma is initially produced by ECH and then expanded with increasing stored energy W_p due to NBI heating. For the TD plasma, the line-averaged electron density $\overline{n}_e$ reaches its maximum shortly after the termination of the gas puffing, and the OV/CIII emission and P_{rad} are roughly proportional to $\overline{n}_e$ up to 0.88s. Then, with further decrease in temperature, a sharp increase is shown in OV/CIII radiation. But their amount is small, having little contribution to P_{rad}. In the RC shot, the strong gas puffing results in a continuous increasing of $\overline{n}_e$ and thus increases in OV/CIII emission and P_{rad}. After 0.86s, the highly increased $\overline{n}_e$ induces a dramatic nonlinear increase of P_{rad} with $\overline{n}_e$, implying the occurrence of a thermal

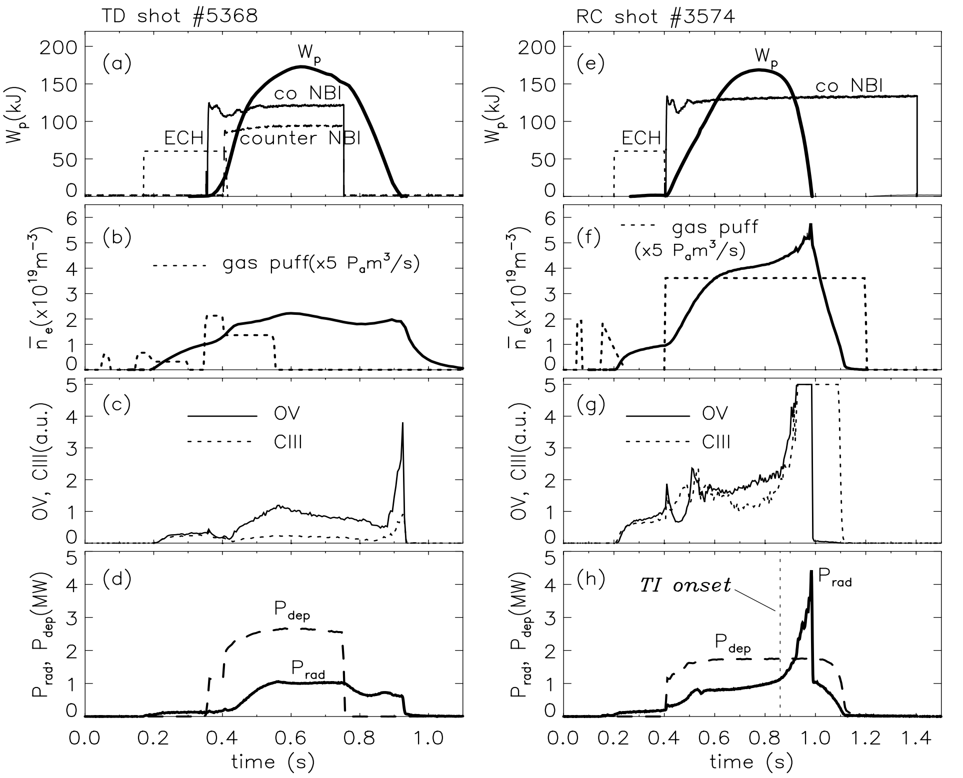

Fig. 1. Typical discharge waveforms of a thermal decay(TD) (left column) and a radiative collapse(RC) (right column) discharge. (a) and (e) Total plasma stored energy, ECH and NBI timing, (b) and (f) line-averaged density and gas puff, (c) and (g) emission intensity of OV and CIII and (d) and (h)total radiated power and deposited NBI power. The dashed line in (h) indicates a TI onset.

instability(TI). In Fig.1, we can also see that the P_{rad} in the TD plasma is smaller than P_{dep} (deposited NBI power) during the NBI phase, while for the RC plasma, P_{rad} is increased rapidly after the TI onset and exceeds P_{dep} soon, leading to a collapse of the discharge. The above results reveal a crucial role of the density level in dominating the decay and collapse of the discharge. On LHD, another clear difference between the TD and RC plasmas lies in their total radiation structures. Fig. 2 displays the contour plots of the time evolution of the chord-integrated radiation brightness for the TD and RC shots shown in Fig. 1. In Fig. 2(a), the TD plasma shows a symmetric radiation profile on the inboard-outboard side throughout the discharge, while in Fig. 2(b) the RC plasma shows a symmetric radiation profile at the first stage and then an asymmetric profile with high radiation located on the inner side of the torus before the end of the discharge. As seen in the expanded time trace, the asymmetric radiation(AR) occurs at about 0.935s, roughly 80ms later than the TI onset, as shown by the dashed line in Fig. 1(h).

4. Characterization of the poloidally asymmetric radiation in RC discharges

As seen in Fig. 2(b), the basic property of the AR on LHD resembles that of MARFE observed in tokamaks, which also radiates stronger on the inner side. But unlike MARFE, the AR on LHD is transient and only appears before the end of the RC discharge. A similar time evolution in the density profile has been observed[7]. Here we focus on the comparisons of the time evolutions of the radiation profile with those of the temperature and temperature profile. shown in Fig. 3 is another RC shot summary. In Fig. 3(a), the sudden nonlinear increase of P_{rad} with $\bar{n}_e$ at 1.64s indicates a TI onset. Fig. 3(b) displays that the initial drop of central temperature T_{e0} occurs at ~1.3s, considerably earlier than the TI onset time. In Figs. 3(c) and (d), an expanded time trace of T_{e0} is shown together with the radiation brightness contour plot, where the AR is observed beginning at 1.75s. Thus, the collapse of T_{e0} can be divided into three phases: phase I before TI onset, phase II between TI and AR and phase III after AR formation. In Fig. 4, the electron temperature T_e profiles

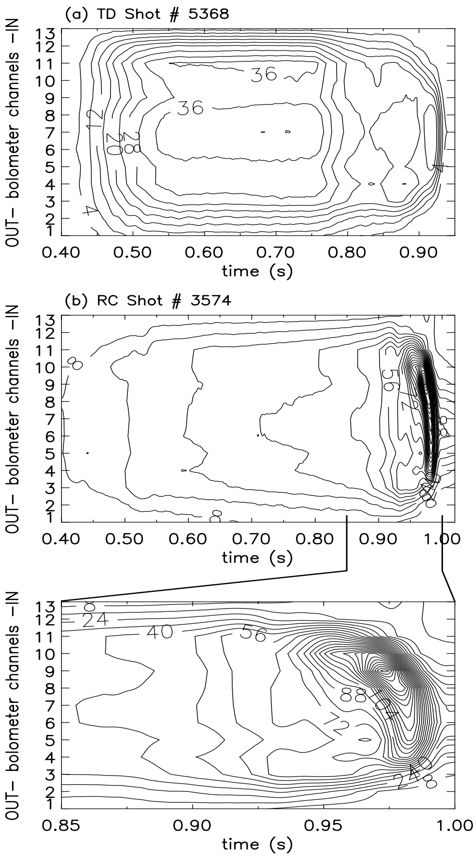

Fig. 2 Contour plots of the time evolution of the chord-integrated radiation brightness for the TD and RC shots shown in Fig. 1

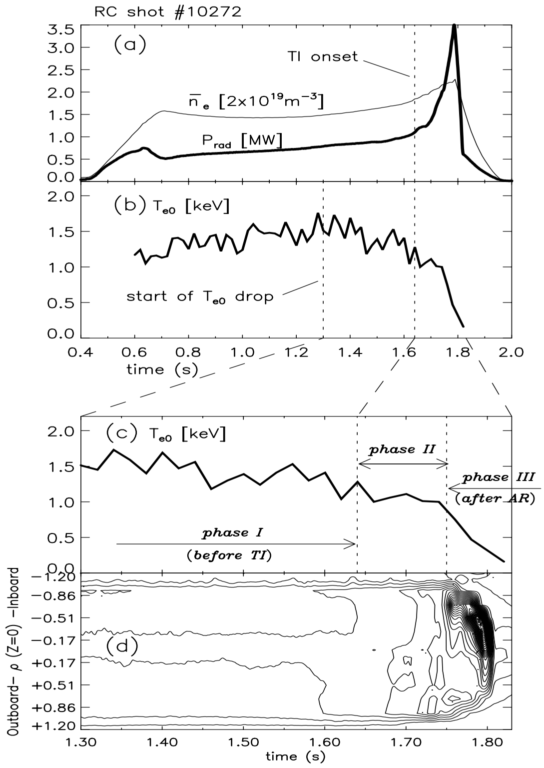

Fig. 3. Time traces of (a) line-averaged density $\bar{n}_e$ and total radiated power P_{rad} and (b) central electron temperature T_{e0} during a RC shot. Shown in (c) is the expanded time trace of T_{e0} and (d) the contour plot of the chord-integrated radiation brightness.

measured at four times(t1 ,t2, t3, t4) across the above three phases are plotted in terms of the normalized radius ρ. From this figure, we can see that in phase I (t1-t2) the overall T_e profile is reduced to a low level. From the beginning of phase II (t2-t3), a clear shrinking of the plasma radius can be observed, indicating that a substantial contraction of the plasma is initiated after the trigger of TI. But unlike that in tokamaks, this shrinkage of plasma does not result in any sudden dramatic termination of the discharge. In phase III (t3-t4), with the plasma column further contracting, the differences between the inboard and outboard T_e profiles at the edge zone are rather clear. On the outer periphery (below dashed line, $T_e \leq 50$eV), the T_e on the inner side is lower than outside, consistent with the asymmetric radiation profile, i. e., low temperature, high radiation on the inner side and high temperature, low radiation on the outer side. The results indicate a good coincidence of the development of the radiation profile with the temperature and density profiles.

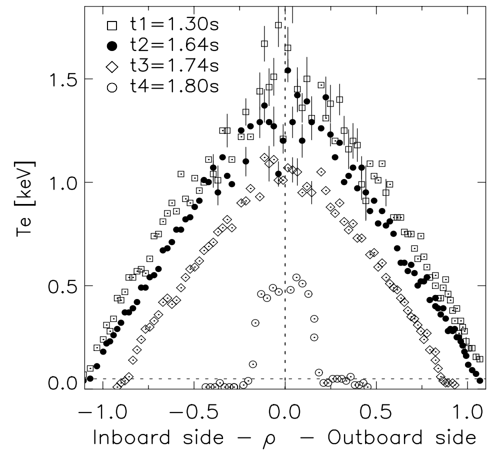

Fig. 4. Electron temperature T_e profiles measured at four times across the three temperature collapse phases I, II and III, as shown in Fig.3

5. Summary

In this paper, the TD(thermal decay) and RC(radiative collapse) discharges on LHD have been reported. Comparisons between them indicate that the density limit processes play a crucial role in dominating the decay and collapse of the discharge. The different features in their radiation profiles are also shown. In the RC discharges, the total radiation profile develops in several phases, consistent with the time evolutions of temperature and density profiles. A shrinkage of the plasma column is observed just after the onset of TI.

References:

[1] Rapp, J., et al., Nucl. Fusion **39** (1999) 765.

[2] Sudo, S., et al., Nucl. Fusion **30** (1990) 11.

[3] Ohyabu, N., Nucl. Fusion **9** (1979) 1491; Stacey, W. M., Phys. Plasmas **4** (1997) 1069.

[4] Lipschultz, B., J. Nucl. Mater. **145-147** (1987) 15.

[5] Giannone, L., et al., Plasma Phys. Control. Fusion **42** (2000) 603.

[6] Itoh, K., Itoh, S.-I., Giannone, L., Research Report NIFS-627(2000).

[7] Peterson, B.J., et al., submitted to Phys. Plasmas.